Variation of 5*d*-level position and emission properties of BaF_2:Pr crystals

P. A. Rodnyi,[1] G. B. Stryganyuk,[2] C. W. E. van Eijk,[3,*] and A. S. Voloshinovskii[4]
[1]*St. Petersburg State Polytechnical University, Polytekhnicheskaya 29, 195251 St. Petersburg, Russian Federation*
[2]*HASYLAB at DESY, Notkestr. 85, 22607 Hamburg, Germany*
[3]*Delft University of Technology, Mekelweg 15, 2629 JB Delft, The Netherlands*
[4]*Ivan Franko National University of Lviv, Kirilo i Mefodii 8, 290005 Lviv, Ukraine*
(Received 19 May 2005; published 23 November 2005)

The emission and excitation spectra of BaF_2 doped with 0.3 and 3.0 mol % Pr^{3+} have been studied using synchrotron radiation in the range from 5 to 30 eV. In BaF_2:Pr^{3+} (0.3 mol %) the lowest level of the $4f5d$ configuration of Pr^{3+} is located at 5.55 eV relative to the $^3H_4,4f$ ground state. The $^1S_0,4f$ level lies higher, at 5.77 eV. Consequently the crystal shows two types of the Pr^{3+} emissions, one related to $5d \rightarrow 4f$ transitions with a decay constant of 22 ns, another related to slow transitions from the $^3P_0$ level. In BaF_2:Pr^{3+} (3.0 mol %) the lowest $5d$ state lies at 6.0 eV, that is above the $^1S_0$ level. At 10 K the crystal shows cascade emission, i.e., $^1S_0 \rightarrow {}^1I_6$ transitions followed by transitions from the $^3P_0$ level. At room temperature the second step of the cascade is quenched. It is shown that the energy shift of the $5d$ state as a function of Pr^{3+} concentration is due to the formation of Pr^{3+}-based clusters at higher concentrations.

DOI: 10.1103/PhysRevB.72.195112 PACS number(s): 78.60.−b, 78.55.−m, 29.40.Mc

I. INTRODUCTION

The position of the excited $5d$ levels of trivalent rare-earth ions (R^{3+}) in inorganic compounds strongly affects the luminescence properties of phosphors.[1] Particularly, the lowest level of the $4f5d$ configuration of the Pr^{3+} ion in a compound with a weak crystal field can be located just above the $^1S_0$ level of the $4f$ configuration enabling cascade emission of two photons by the activator ion.[2,3] Photon cascade emission (PCE) attracts considerable interest owing to the possibility of obtaining two visible photons from excitation by one ultraviolet photon and a quantum efficiency of the phosphors greater than unity. When the condition $E(5d) > E(^1S_0,4f)$ is met in a crystal, two cases are possible. The fist one represents the most important group of crystals offering PCE, which we denote as group 1*a*. In this case, the first step of the cascade corresponds to $^1S_0 \rightarrow {}^1I_6$ transitions (emission line near 400 nm) and the second step is related to transitions from the $^3P_0$ level to different lower levels (emission wavelength longer than 470 nm). In another case (group 1*b*) only the $^1S_0$ luminescence, i.e., the first step of PCE is observed. One explanation for the absence of emission from the $^3P_0$ level is multiphonon relaxation. This is in particular typical for borate crystals, which offer high phonon frequencies.[4] Another explanation of $^3P_0$ luminescence quenching is cross-relaxation. This occurs at a high concentration of the activator (Pr^{3+}). For instance, LaF_3:Pr (~1%) is a good PCE phosphor,[5] while PrF_3 shows only $^1S_0$ luminescence.[6] Finally, in a rich variety of compounds (group 2) the crystal field for Pr^{3+} is so strong that $E(5d) < E(^1S_0,4f)$ and $5d \rightarrow 4f$ emission and/or transitions from the $^3P_0$ level are detected.

The maximum luminescence intensity of Pr^{3+}-doped crystals with fluorite structure is usually detected for the activator content at a level of several tenths of an atomic percent. That is why BaF_2 crystals doped with low Pr concentration (~0.1%) were studied.[7,8] In this work it is shown that BaF_2:Pr can belong to group 1 or group 2 depending on the concentration of the activator. At low activator concentration ($\leqslant$0.3 mol %) radiative transitions from the $4f5d$ configuration and $^3P_0,4f$ level are observed, while at 3.0 mol % of Pr^{3+} the $^1S_0 \rightarrow {}^1I_6$ transitions predominate. This phenomenon is related to creation of Pr-based clusters in barium fluoride at high activator concentration.

II. EXPERIMENTAL

BaF_2:Pr single crystals were grown at the St. Petersburg State Optical Institute using the modified Bridgman technique. Good quality transparent samples with dimensions of about $3 \times 6 \times 8$ mm^3 were used in the measurements. In this study we examined two crystals of BaF_2:Pr with activator concentration of 0.3 and 3.0 mol %. The activator concentration in BaF_2 was chosen based on the following arguments. It has been shown by different methods that R^{3+} ions introduced in fluorite-structure crystals may form clusters containing six activator ions ($[R_6F_{37}]$ clusters).[9] The clustering process begins when the R content exceeds several tenths of a percent. Total clustering is reached at several percent of R^{3+} in MF_2 (M=Ca,Sr,Ba,Cd). At a R content of about 10% the clusters may coagulate forming larger structural units.[10] On the other hand, the maximum luminescence intensity of "isolated" centres of Pr^{3+} (Ref. 8) and Ce^{3+} (Ref. 11) is reached for ~0.2 mol %-doped BaF_2. Thus, we undertook the investigation of a BaF_2:Pr (3.0 mol %) sample anticipating that this crystal contains basically the $[Pr_6F_{37}]$ clusters, and a sample with the tenfold less content (0.3 mol %) of Pr^{3+} for an understanding of the properties of the isolated Pr^{3+} centres.

Preliminary measurements of the emission spectra were carried out under x-ray excitation; the results were reported quite recently.[12] Measurements of luminescence excitation and emission spectra as well as decay kinetics were performed at the Deutsches Elektronen Synchrotron (DESY,

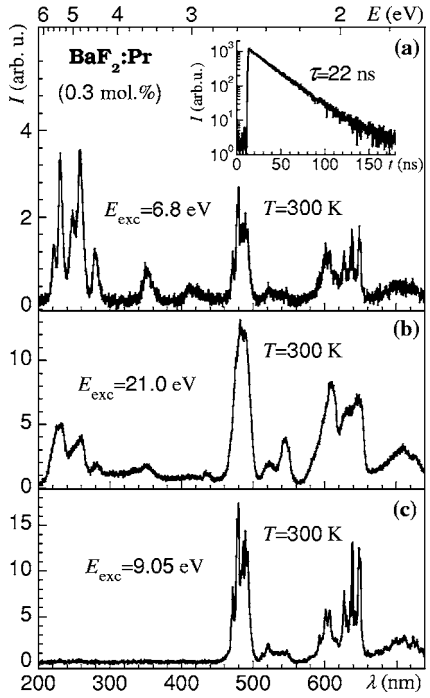

FIG. 1. Emission spectra of BaF_2:Pr (0.3 mol %) excited by photons with energy (a) 6.8 eV, (b) 21.0 eV, and (c) 9.05 eV. Inset: decay curve for the 255-nm emission band. $T=300$ K.

Hamburg) using the facility of SUPERLUMI station at HASYLAB. The measurements were carried out at 300 and 10 K. Emission spectra were measured in the range from 200 to 900 nm with a resolution of about 1 nm using an ARC "Spectra Pro 308" 30 cm monochromator-spectrograph in Czerny-Turner mounting equipped with a Princeton Instruments CCD detector. The emission spectra were not corrected for the detector sensitivity and monochromator transmission.

Time resolved luminescence excitation spectra were scanned from 5 to 30 eV with a resolution of 0.32 nm by the primary 2 m monochromator in 15° McPherson mounting, using a HAMAMATSU R6358P detector at the secondary ARC monochromator. Integrated excitation spectra correspond to the total signal formed by the photomultiplier. Fast and slow components were monitored after the excitation pulse within a time gate of 0–5 ns and 100–180 ns, respectively. The luminescence excitation spectra were corrected for the incident photon flux.

III. RESULTS

A. BaF_2:Pr (0.3 mol %)

Emission spectra of BaF_2:Pr (0.3 mol %) are presented in Fig. 1. Under direct excitation of Pr^{3+} ions [Fig. 1(a)] the sample shows several bands clustered in range from 200 to 300 nm and a number of long wavelength lines. A similar spectrum was detected earlier in BaF_2:Pr^{3+} (0.2 mol %).[8] The decay-time constant of the short-wavelength emissions is 22 ns [inset of Fig. 1(a)], which is typical for the $5d\rightarrow 4f$ transitions of Pr^{3+} ions. The emissions near 480 and around 600 nm are related to transitions from the $^3P_0$ level of Pr^{3+}, i.e., so-called $^3P_0$ luminescence.

It is common knowledge that pure BaF_2 shows two types of intrinsic luminescence. If the energy of the incident photons ($h\nu_{exc}$) exceeds ~9.5 eV self-trapped exciton (STE) luminescence is observed, that is a wide emission band peaking at 310 nm.[13] At $h\nu_{exc}>18$ eV core-valence luminescence with a main band at 220 nm can be detected in BaF_2.[14] The emission spectrum under 21-eV photon excitation [Fig. 1(b)] has been measured to test the availability of the intrinsic luminescence in BaF_2:Pr (0.3 mol %). One can see that the spectrum contains short wavelength bands at 230 and 259 nm attributed to $5d\rightarrow 4f$ emission and a number of lines in the long wavelength region, which can be related to transitions from the $^3P_0$ level of Pr^{3+}. Weak STE luminescence is present in the spectrum of Fig. 1(b) (broad band around 300 nm).

Thus under $4f\rightarrow 5d$ [Fig. 1(a)] and band-to-band [Fig. 1(b)] excitations the crystal shows efficient $5d$ and $^3P_0$ luminescence. Consequently the sample belongs to the group 2 crystals. In the region around 9 eV, where the incident photon energy is above those of the $4f\rightarrow 5d$ excitation but below the band-to-band transition region, the $^3P_0$ luminescence predominates [Fig. 1(c)].

Taking into consideration that the $4f$ level positions do not essentially depend on the host crystal one can identify the detected spectral lines. The main short-wavelength emission lines of BaF_2:Pr (0.3 mol %) are associated with transitions from the lowest state of the $4f5d$ configuration to $^3H_4$ (230 nm), $^3H_6$ (257 nm), and $^3F_4$ (280 nm) levels of the $4f$ configuration. The most intensive long wavelength lines belong to transitions from the $^3P_0$ level to the $^3H_4$ (484 nm), $^3H_6$ (600 nm), and $^3F_2$ (640 nm) levels.

The excitation spectra of BaF_2:Pr (0.3 mol %) emission are presented in Fig. 2. For 255-nm emission two intense wide excitation bands peaking at 6.1 and 7.5 eV have been detected [Fig. 2(a)]. Both bands belong to the $4f\rightarrow 5d$ transitions; the onset of the transitions is located at 5.5 eV. The expected five-band structure, which is observed in some Pr-doped crystals,[15] does not show up here. A low intense band at 9.5 eV can be attributed to exciton creation in BaF_2. At higher energies band-to-band transitions occur. The forbidden band width (E_g) of BaF_2 is 10.6 eV at room temperature.

The integral [curve 1, Fig. 2(a)] as well as fast [curve 2, Fig. 2(a)] components of the $5d$ luminescence show an increase in intensity at $h\nu_{exc}>18$ eV, that is in the region of excitation of $5p$Ba core states. The mechanism of energy transfer from the core (cation) excitations to luminescence centres in BaF_2 has been described elsewhere.[14] In the region from 9 to 18 eV the slow [curve 3, Fig. 2(a)] component is very similar to the integral one [curve 1, Fig. 2(a)]. It means that the energy transfer from excitons (9.5-eV peak) and electron-hole pairs ($h\nu_{exc}>10$ eV) represents a slow process going on with a delay.

The excitation spectrum of the 485-nm luminescence is presented in Fig. 2(b). The spectrum shows three intense bands 6.85, 8.3, and 9.1 eV at $h\nu_{exc}<E_g$ and a rise of the intensity in the region of the band-to-band transitions. The excitation spectrum of the 640-nm emission shows a similar

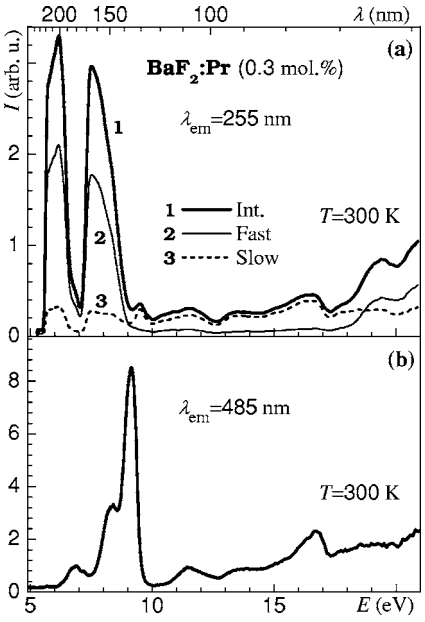

FIG. 2. Excitation spectra of (a) 255-nm and (b) 485-nm emission of BaF_2:Pr (0.3 mol %) at 300 K.

shape, so the spectrum in Fig. 2(b) reflects common properties of the $^3P_0$ luminescence.

B. BaF_2:Pr^{3+} (3.0 mol %)

Emission spectra of BaF_2:Pr^{3+} (3.0 mol %) are essentially different (Fig. 3) from those of the low-concentrated crystal. The low-temperature spectrum under $4f \rightarrow 5d$ excita-

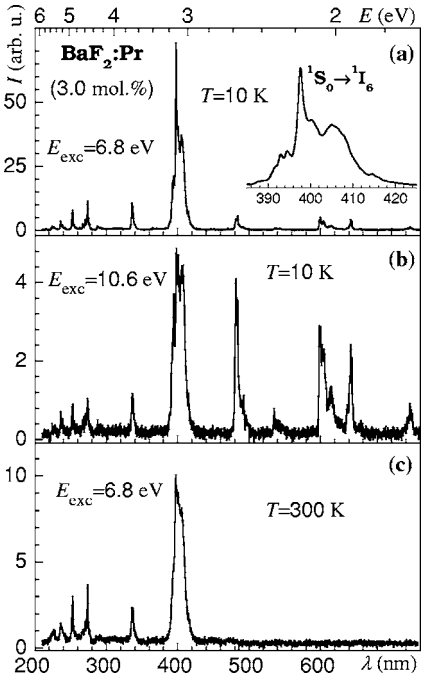

FIG. 3. Emission spectra of BaF_2:Pr (3.0 mol %) excited by photons with energy: (a),(c) 6.8 eV and (b) 10.6 eV measured at (a),(b) 10 K and (c) 300 K.

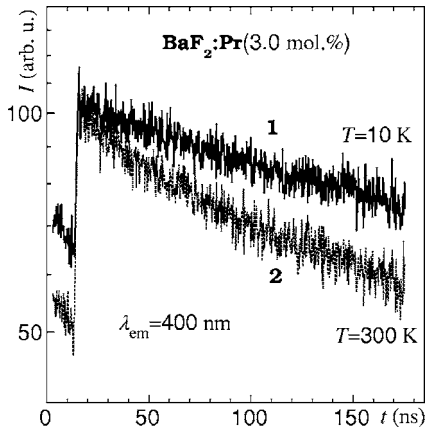

FIG. 4. Decay kinetics curves of BaF_2:Pr (3.0 mol %) excited by 6.89-eV quanta and detected near 400 nm ($^1S_0 \rightarrow {}^1I_6$ transitions) at (1) 10 K and (2) 300 K.

tion [Fig. 3(a)] shows PCE with an intense first step, that is the 397.2 nm line from the $^1S_0 \rightarrow {}^1I_6$ transition, and a rather weak second step, i.e., emission at $\lambda > 450$ nm. For comparison, the $^1S_0 \rightarrow {}^1I_6$ line is located at ~400 nm in YF_3:Pr (Ref. 6) and at 394 nm in LaF_3:Pr.[16] The short wavelength emission lines at 215.4, 223.8, 238.8, 252.6, 273.8, and 335.4 nm are related to transitions from the $^1S_0$ state to the $^3H_4$, $^3H_5$, $^3H_6$, $^3F_4$, $^1G_4$, $^1D_2$ levels, respectively (one-photon $^1S_0$ luminescence). The inset in Fig. 3(a) shows the $^1S_0 \rightarrow {}^1I_6$ emission in more detail.

At 10 K the second step of PCE is more distinct under excitation in the fundamental region of BaF_2 absorption [Fig. 3(b)]. The spectrum shows a less intense first step of PCE and the following long wavelength lines: 484.0 nm ($^3P_0 \rightarrow {}^3H_4$), 537.5 nm ($^3P_0 \rightarrow {}^3H_5$), 600.1 nm ($^3P_0 \rightarrow {}^3H_6$), 642.3 nm ($^3P_0 \rightarrow {}^3F_2$), and 725.7 ($^3P_0 \rightarrow {}^3F_4$).

At 300 K under $4f \rightarrow 5d$ excitation only the $^1S_0$ luminescence is efficient with the main $^1S_0 \rightarrow {}^1I_6$ line at 396.3 nm [Fig. 3(c)]. The long wavelength emission (>450 nm) is negligible in BaF_2:Pr^{3+} (3.0 mol %). The room-temperature spectrum of BaF_2:Pr^{3+} (3.0 mol%) is similar to that of PrF_3 (Ref. 6) and this allows us to suppose that the emission of the former one is related to Pr-based clusters. Thus, BaF_2:Pr^{3+} (3.0 mol %) shows properties of group 1*a* at low temperature and group 1*b* at room temperature.

The decay kinetics curves of the $^1S_0 \rightarrow {}^1I_6$ line of BaF_2:Pr^{3+} (3.0 mol %) are presented in Fig. 4. The decay constants (τ) are 490 ns at 10 K and ~400 ns at room temperature. The value of τ tends to grow with increasing energy of the incident photons: $\tau = 570$ ns at $h\nu_{exc} = 8.0$ eV, and $\tau = 710$ ns at $h\nu_{exc} = 9.92$ eV ($T = 10$ K). For reference, $\tau = 530$ ns in YF_3:Pr (300 K),[6] and $\tau = 730$ ns in LaF_3:Pr (20 K).[5] The time characteristics of the $^3P_0$ luminescence were not determined because of the too long decay time of a few microseconds.

Figure 5 presents the excitation spectra of the $^1S_0 \rightarrow {}^1I_6$ emission of BaF_2:Pr^{3+} (3.0 mol %) at 10 and 300 K. The low-temperature spectrum (curve 1) shows two most intensive bands peaking at 6.84 and 7.48 eV which are related to the $4f \rightarrow 5d$ transitions, the onset of the transitions is located

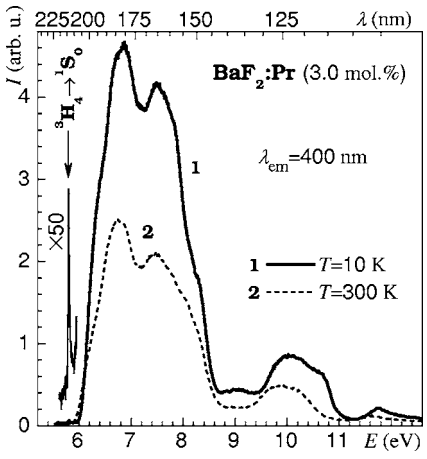

FIG. 5. Excitation spectra of the 400-nm emission of BaF_2:Pr (3.0 mol %) at (1) 10 K and (2) 300 K.

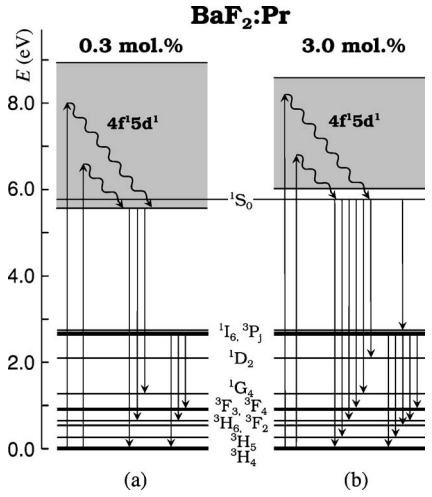

FIG. 6. Energy levels and the strongest transitions of Pr^{3+} in (a) BaF_2:Pr (0.3 mol %) and (b) BaF_2:Pr (3.0 mol %).

at 6.0 eV. The low and high-energy bands belong to the transitions to the doublet e_g and triplet t_{2g} states of the $4f5d$ configuration, respectively.[1] A band around 10 eV may be associated with the creation of excitons and band-to-band transitions in barium fluoride.[17] Furthermore, a rise in the excitation spectrum was observed above 20 eV (not shown). The low-temperature spectrum clearly shows the $^3H_4 \rightarrow {}^1S_0$ transitions at 214.6 nm (5.77 eV; magnified curve of Fig. 5). The positions of the corresponding lines in $YF_3:Pr^{3+}$ and $LaF_3:Pr^{3+}$ are almost the same: 215 nm at 300 K (Ref. 6) and 213.4 nm at 20 K,[5] respectively. The room-temperature spectrum (curve 2, Fig. 5) shows similar $5d$ bands peaking at 6.74 and 7.49 eV with an onset at 5.9 eV. It means that at 300 K the energy gap between the lowest $5d$ state and the $^1S_0$ level is rather small, 0.13 eV.

IV. DISCUSSION

The obtained data show that at low activator concentration BaF_2:Pr contains the isolated Pr^{3+} centers; the crystal produces $5d$ and $^3P_0$ luminescence (Figs. 1 and 2) and shows emission properties of group 2 crystals. The presence of the $^1S_0$ luminescence (Fig. 3) in $BaF_2:Pr^{3+}$ (3.0 mol %) suggests that the $^1S_0$ state is located below the states of the $4f5d$ configuration, as follows also from the excitation spectrum (Fig. 5). An energy-level diagram of the studied crystals can be constructed on the basis of the obtained emission and excitation spectra (Fig. 6). In BaF_2:Pr (0.3 mol %) the lowest $5d$ level is located at 5.55 eV and $5d \rightarrow 4f$ transitions are efficient [Fig. 6(a)]. In BaF_2:Pr (3.0 mol %), the lowest $5d$ state lies at 6.0 eV, that is above of the $^1S_0$ level [Fig. 6(b)]. After $4f \rightarrow 5d$ excitation, the system nonradiatively relaxes to the $^1S_0$ level owing to the rather small $5d$-$^1S_0$ gap, 0.23 eV at 10 K. Then the first step of PCE, i.e., $^1S_0 \rightarrow {}^1I_6$ emission occurs. Subsequently the system again nonradiatively relaxes to the $^3P_0$ level and the second step of PCE takes effect.

The absence of a structure in the two $5d \rightarrow 4f$ excitation bands of BaF_2:Pr (0.3 mol %) [Fig. 2(a)] indicates that the $5d$ states of Pr^{3+} in BaF_2 are located in the conduction band of the crystal. According to Ref. 18, the lowest $5d$ level of Pr^{3+} in BaF_2 lies near the bottom of the conduction band.

The emission properties of BaF_2:Pr (0.3 mol %) are mainly as expected, but the $^3P_0$ luminescence excitation spectrum [Fig. 2(b)] possesses some peculiarities. In some compounds the $^3P_0$ level can be fed from STE. For instance energy transfer from STE to Pr^{3+} ($^3H_4 \rightarrow {}^3P_0$) was observed in $SrAlF_5$:Pr.[3] In BaF_2:Pr (0.3 mol %) three main excitation bands are located in the sub-excitonic region [Fig. 2(b)] and excitons with a maximum energy of 9.8 eV (Ref. 17) cannot be involved in this process. One can find some elements of anticorrelation between excitation of the $^3P_0$ luminescence [Fig. 2(b)] and $5d$ luminescence [Fig. 2(a)]: the onset of the former at 6.2 eV corresponds to the beginning of the first drop of the latter; the first maximum of the former at 6.85 eV is close to the minimum of the $5d$ luminescence at ~7.0 eV; the maximum of the $^3P_0$ luminescence near 9.1 eV is located in the region of the minimum of the $5d$ luminescence. So the intensity of the $^3P_0$ luminescence increases as the intensity of the $5d$ luminescence decreases. Such an anticorrelation points to a competition process in the population of $5d$ and $^3P_0$ states. It can be suggested that when the probability of the $5d \rightarrow 4f$ emission decreases [minima in the curve of Fig. 2(a)], the excitons created in the vicinity of Pr^{3+} ions are involved in the process.[3,11] The energy of the activator-bound excitons is large enough for population of $^3P_0$ states, but not for $^1S_0$ states.

$BaF_2:Pr^{3+}$ (3.0 mol %) shows PCE at low temperature [Figs. 3(a) and 3(b)], while at room temperature the $^1S_0$ luminescence predominates [Fig. 3(c)]. One can see that the emission spectra of $BaF_2:Pr^{3+}$ (3.0 mol %), presented in Figs. 3(a) and 3(b), differ in intensity. The point is that at $4f \rightarrow 5d$ excitation [Fig. 3(a)] intercenter emission occurs, while at band-to-band excitation [Fig. 3(b)] we deal with recombination luminescence.

The strong quenching of the second step of PCE of $BaF_2:Pr^{3+}$ (3.0 mol %) compared with $BaF_2:Pr^{3+}$ (0.3 mol %) suggests an interaction between Pr^{3+} ions in the former one. The Pr^{3+} ions can approach close enough for the interaction to be sufficiently strong and cross-relaxation oc-

curs. So the depopulation of the $^3P_0$ level is effected by the cross-relaxation process $(^3P_0, ^3H_4) \rightarrow (^1G_4, ^1G_4)$, which is possible owing to closely related energy gaps between corresponding levels (Fig. 6). It has been shown that cross relaxation in LaF_3:Pr is efficient on very short distance (~4 Å) between Pr^{3+} neighbors.[19] The estimated average distance between the Pr^{3+} ions at their uniform distribution in BaF_2:Pr^{3+} (3.0 mol %) is 12.5 Å and the distance between nearest neighbour Ba^{2+} sites in BaF_2 is 4.38 Å. In view of this, we may argue that the strong concentration quenching of the $^3P_0$ luminescence is the result of formation of Pr-based clusters in the BaF_2 lattice. The absence of the $^3P_0$ luminescence in BaF_2:Pr^{3+} (3.0 mol %) at room temperature, shows that the cross-relaxation process is supplemented by thermal quenching.

We can now consider the studied processes on general grounds. The energies of 5*d* states of R^{3+} ions in a compound compared with those of free ions reduce with increasing interaction of the 5*d* electron with the neighbouring anion ligands. The energy depression $D(R^{3+})$ of the lowest 5*d* level or so-called spectroscopic redshift in a compound tends to decrease with increasing anion coordination number (N). For the well-studied Ce^{3+} ion, the redshift $D(Ce^{3+})$ is 14 640, 9915, and 8750 cm^{-1} in BaF_2 ($N=8$), YF_3 ($N=9$), and LaF_3 ($N=11$), respectively.[20] As found by Dorenbos,[20] the redshift is approximately the same for all R^{3+} ions in a given compound. Then taking into account that the energy of the first $4f \rightarrow 5d$ transition of a free Pr^{3+} ion is 61 580 cm^{-1}, one can find the position of the lowest 5*d* level $E(5d)$ of Pr^{3+} in BaF_2, YF_3, and LaF_3 at 46 940, 51 660, and 52 830 cm^{-1}, respectively. The excited $^1S_0$ level of the 4*f* configuration lies at around 47 000 cm^{-1} above the ground state and deviates only slightly depending on the compound, owing to strong shielding of the 4*f* orbital. Consequently the emission from the $^1S_0$ level cannot be observed in BaF_2:Pr (in case of low concentration) because $E(5d) < E(^1S_0, 4f)$ [Fig. 6(a)]. Thus, the obtained characteristics of the BaF_2:Pr (0.3 mol %) are in agreement with the relevant data. In YF_3:Pr and LaF_3:Pr the $^1S_0$ level lies below the 5*d* states and the conditions for $^1S_0$ luminescence and PCE are met.[5,6]

The value $D(R^{3+})$ depends also on the size and shape of the anion coordination polyhedron, covalency and anion polarizability (see Refs. 1 and 21 for details). For low covalency (fluorides) the redshift increases with increasing average distance R_{av} of the cation to the N coordinating anions and distortion of the polyhedron.[20,21] The Pr^{3+} ion in BaF_2 occupies a barium site which has a cubic coordination of eight fluorine ions. The excess charge of the Pr^{3+} ion in a divalent cation site needs to be compensated. In BaF_2 this occurs by means of an extra F^- ion preferably located at a next-nearest-neighbor site along the ⟨111⟩ direction producing C_{3v} symmetry.[22] So, the Pr^{3+} ions in the BaF_2 lattice at low concentration have an eightfold coordination with small distortion which offers a large redshift. On the other hand, barium fluoride has a large average distance $R_{av}=2.69$ Å implying a weak crystal field. However, it has been shown theoretically and confirmed experimentally that in BaF_2:Ce the distance to the nearest neighbours decreases by 10% owing to the larger charge of Ce^{3+} compared with the barium ion.[21] The eight fluorine ions surrounding the Pr^{3+} ion in BaF_2:Pr should be involved in a similar process resulting in a Pr^{3+}-F^- distance smaller than R_{av} in BaF_2. In addition the ionic radius of Pr^{3+}, 1.28 Å, is less than that of Ba^{2+}, 1.56 Å (for $N=8$ and fluorine surrounding).

An increase of the Pr^{3+} concentration results in extra F^- ions located in nearest interstitial sites (C_{4v} center) and coming together of Pr^{3+} ions due to their coagulating tendency.[10] As a result clusters with ninefold coordinated Pr^{3+} ions begin to form in BaF_2:Pr at an activator content exceeding about 0.5 mol %. The lowest 5*d* level goes up and the main condition for detection of the $^1S_0$ luminescence $E(5d) > E(^1S_0, 4f)$ becomes valid in highly concentrated BaF_2:Pr [Fig. 6(b)]. Notice that the rise of the lowest 5*d* level with increasing Pr^{3+} concentration has been observed recently in the $K_5Li_2La_{1-x}Pr_xF_{10}$ compound.[23]

The existence of clusters with ninefold coordinated Pr^{3+} in BaF_2:Pr (3.0 mol %) is confirmed by the following points.

(1) The onset (6.0 eV) of the $4f \rightarrow 5d$ excitation band or the position of lowest 5*d* level in the crystal [Fig. 5(a)] is quite similar to that in YF_3:Pr (0.1%) (Ref. 6), where $N=9$ for Pr^{3+}. In LaF_3:Pr the 5*d* onset lies at 6.2 eV.[5] The detected two excitation bands peaking at 6.84 and 7.48 eV [Fig. 5(a)] are similar to the corresponding bands of YF_3:Pr (0.1%), however, the latter show a structure. In LaF_3:Pr a wide nonstructural band was detected.[5]

(2) The emission from the $^3P_0$ level is weak at 10 K and almost completely quenched at 300 K. This quenching is caused by a strong cross-relaxation process between Pr^{3+} ions, which is effective at small distances between the ions as it occurs in the clusters.

(3) The crystal field splitting of the 5*d* states, the so-called 10 Dq value in cubic coordination, should be bigger than that in a trigonal prism with caps on the three rectangular faces, as for Pr^{3+} in YF_3, or in a five-capped trigonal prism, as for Pr^{3+} in LaF_3.[20] The total width of the $4f \rightarrow 5d$ excitation bands, 2.6 eV, which reflects the crystal field splitting, is approximately the same in BaF_2:Pr (3.0 mol %) and in YF_3:Pr (Ref. 6) indeed, while in BaF_2:Pr (0.3 mol %) this value is 3.4 eV [Fig. 2(a)].

Notice that the formation of the R-based clusters is a special feature of fluoritelike crystals. The point is that the fluorite lattice is rather loose (many voids), this is in particular true for BaF_2 where ions fill only 52% of the space (in the approximation of rigid spheres). A R^{3+} activator occupies a M^{2+} cation site of the fluorite lattice and the excess activator charge is neutralised by an F^- ion displaced to the void of fluorine cube (interstitial site). The fluorine-cube voids are favorable also to migration of the R^{3+} ions through the lattice. Eventually, the formation of a more dense packing structure is energetically advantageous, and rare earth $[R_6F_{37}]$ clusters are formed.[9,10] In calcium fluoride the cluster formation is essentially efficient for dopants with small ionic radius, and CaF_2 with $[Y_6F_{37}]$ clusters is such a case.[9] The ratio of the ionic radii of Pr^{3+}/Ba^{2+}, 0.82, is less than that of Y^{3+}/Ca^{2+}, 0.92, and this is convenient for the clustering process in barium fluorite with high concentration of praseodymium. The $[R_6F_{37}]$ clusters of nanometer dimen-

sions can be considered as nanocrystals in the fluoritelike lattice. An important point is that the nanocrystals in the compounds with fluorite structure are formed naturally, i.e., the crystals are not subjected to any additional thermal treatment.

V. CONCLUSIONS

In BaF_2:Pr (0.3 mol %) the lowest $5d$ level lies at 5.55 eV that is below the $^1S_0$ level located at 5.77 eV. The crystal containing isolated Pr^{3+} centres produces $5d$ and $^3P_0$ luminescence, i.e., displays emission properties of group 2 crystals. At an incident photon energy around 9.0 eV, that is in the region between interconfiguration and band-to-band transitions, the $^3P_0$ luminescence of BaF_2:Pr (0.3 mol %) predominates.

The emission spectra of Pr-doped BaF_2 are changed significantly in going from low (0.3%) to high (3.0%) concentration of the activator. The high-energy shift of the $5d$ lowest level has been first observed in BaF_2:Pr. In BaF_2:Pr (3.0 mol %), the $5d$ state lies at 6.0 eV that is above of the $^1S_0$ level. It is shown that the large energy shift of the $5d$ state with increasing Pr^{3+} concentration is due to formation of $[Pr_6F_{37}]$ clusters in BaF_2 lattice. At 10 K the crystal shows cascade emission or the sequence of the $^1S_0 \rightarrow {}^1I_6$ transitions and transitions from the $^3P_0$ level. Thus, at low temperature the high-concentrated crystal belongs to group $1a$, while at room temperature the first step of the cascade predominates in the crystal, i.e., it shows characteristics of group $1b$ crystals.

The excitation spectra are different for the two samples under study. The total $4f \rightarrow 5d$ excitation band widths are 3.4 and 2.6 eV in BaF_2 (0.3 mol %) and BaF_2 (3.0 mol %), respectively. The obtained emission and excitation spectra represent important proof of cluster creation in the high concentrated BaF_2:Pr crystal, which was observed before in alkaline-earth fluorides by means of other methods. The formation of natural Pr-based nanocrystals in the fluorite-structure compounds opens a new way for obtaining photon cascade emitters. The investigation of the BaF_2:Pr crystals to find the optimum praseodymium concentration will be continued.

ACKNOWLEDGMENTS

We gratefully acknowledge professor A. I. Ryskin and Dr. A. S. Shcheulin from the St. Petersburg State Optical Institute for useful discussion of the results and providing the BaF_2:Pr crystals. This work was partly supported by the DFG Graduiertenkolleg No. 463 of Hamburg University, and its experimental part at DESY has been performed in collaboration with Professor Dr. G. Zimmerer's group within HASYLAB Project No. II-03-023.

*Email address: VANEIJK@iri.tudelft.nl

[1] B. F. Aull and H. P. Jenssen, Phys. Rev. B **34**, 6640 (1986).
[2] E. Van der Kolk, P. Dorenbos, C. W. E. van Eijk, A. P. Vink, C. Fouassier, and F. Guillen, J. Lumin. **97**, 212 (2002).
[3] A. P. Vink, P. Dorenbos, J. T. M. de Haas, H. Donker, P. A. Rodnyi, A. G. Avanesov, and C. W. E. van Eijk, J. Phys.: Condens. Matter **14**, 8889 (2002).
[4] A. Srivastava, D. A. Doughty, and W. W. Beers, J. Electrochem. Soc. **144**, l190 (1997).
[5] L. R. Elias, Wm. S. Heaps, and W. M. Yen, Phys. Rev. B **8**, 4989 (1973).
[6] S. Kück and I. Sokolska, Appl. Phys. A: Mater. Sci. Process. **77**, 469 (2003).
[7] J. K. Lawson and S. A. Payne, Opt. Mater. (Amsterdam, Neth.) **2**, 225 (1993).
[8] W. Drozdowski and A. J. Wojtowicz, J. Alloys Compd. **300–301**, 261 (2000).
[9] S. A. Kazanskii and A. I. Ryskin, Phys. Solid State **44**, 1415 (2002).
[10] B. P. Sobolev, A. M. Golubev, and P. Herrero, Crystallogr. Rep. **48**, 141 (2003).
[11] P. Dorenbos, R. Visser, C. W. E. van Eijk, R. W. Hollander, and H. W. den Hartog, Nucl. Instrum. Methods Phys. Res. A **310**, 236 (1991).
[12] A. S. Potapov, P. A. Rodnyi, S. B. Mikhrin, and I. R. Magunov, Phys. Solid State **47**, 1436 (2005).
[13] R. T. Williams and K. S. Song, J. Phys. Chem. Solids **51**, 679 (1990).
[14] P. A. Rodnyi, Sov. Phys. Solid State **34**, 1053 (1992).
[15] L. van Pieterson, M. F. Reid, R. T. Wegh, S. Soverna, and A. Meijerink, Phys. Rev. B **65**, 045113 (2002).
[16] A. Lezama and C. B. de Araujo, Phys. Rev. B **34**, 126 (1986).
[17] P. A. Rodnyi, M. A. Terekhin, and E. N. Mel'chakov, J. Lumin. **47**, 281 (1991).
[18] P. Dorenbos, J. Phys.: Condens. Matter **15**, 2645 (2003).
[19] J. C. Vail and R. Buission, J. Phys. (France) Lett. **43**, L745 (1982).
[20] P. Dorenbos, Phys. Rev. B **62**, 15640 (2000).
[21] J. Andriessen, P. Dorenbos, and C. W. E. van Eijk, Nucl. Instrum. Methods Phys. Res. A **489**, 399 (2002).
[22] I. V. Murin, A. V. Glukhov, and V. M. Reiterov, Sov. Phys. Solid State **21**, 298 (1979).
[23] P. Solarz, G. Dominiak-Dzik, R. Lisiecki, and W. Ryba-Romanowski, Radiat. Meas. **38**, 603 (2004).